Oxidative Aliphatic C-H Fluorination with Fluoride Ion Catalyzed by a Manganese Porphyrin

Wei Liu *et al.*

Science **337**, 1322 (2012);
DOI: 10.1126/science.1222327

P22590-N16 and the Wittgenstein Prize, and the European Union through the integrating project AQUTE, Siemens Austria, and the City of Vienna. T.K. and E.D. thank the Army Research Office for funding from the Defense Advanced Research Projects Agency Optical Lattice Emulator program, Harvard-MIT CUA, NSF grant DMR-07-05472, Air Force Office of Scientific Research Quantum Simulation Multidisciplinary University Research Initiative (MURI), and the Army Research Office–MURI on Atomtronics.

Supplementary Materials
www.sciencemag.org/cgi/content/full/science.1224953/DC1
Materials and Methods
Supplementary Text
Figs. S1 to S5
References (*34*–*58*)

21 May 2012; accepted 21 August 2012
Published online 6 September 2012;
10.1126/science.1224953

Oxidative Aliphatic C-H Fluorination with Fluoride Ion Catalyzed by a Manganese Porphyrin

Wei Liu,[1] Xiongyi Huang,[1] Mu-Jeng Cheng,[2] Robert J. Nielsen,[2] William A. Goddard III,[2] John T. Groves[1]*

Despite the growing importance of fluorinated organic compounds in drug development, there are no direct protocols for the fluorination of aliphatic C-H bonds using conveniently handled fluoride salts. We have discovered that a manganese porphyrin complex catalyzes alkyl fluorination by fluoride ion under mild conditions in conjunction with stoichiometric oxidation by iodosylbenzene. Simple alkanes, terpenoids, and even steroids were selectively fluorinated at otherwise inaccessible sites in 50 to 60% yield. Decalin was fluorinated predominantly at the C2 and C3 methylene positions. Bornyl acetate was converted to exo-5-fluoro-bornyl acetate, and 5α-androstan-17-one was fluorinated selectively in the A ring. Mechanistic analysis suggests that the regioselectivity for C-H bond cleavage is directed by an oxomanganese(V) catalytic intermediate followed by F delivery via an unusual manganese(IV) fluoride that has been isolated and structurally characterized.

Biochemistry manifests numerous highly selective transformations of aliphatic C-H bonds into alcohols, halides, and olefins catalyzed by reactive metal-oxo intermediates within enzymes (*1*, *2*). A notable exception is aliphatic C-H bond fluorination: The only fluorinase enzymes yet characterized form C-F bonds by nucleophilic displacement at the preactivated C center of *S*-adenosylmethionine (*3*, *4*). There are no catalytic ways to selectively and directly incorporate fluoride ions into unreactive sp^3 C-H bonds. Yet there is an enormous impetus today to place F at such inaccessible sites in biomolecules and drug candidates. Fluorination of drugs can block sites of phase I metabolism by cytochrome P450 enzymes as well as improving target-binding affinities (*5*). Further, the incorporation of ^{18}F into biomolecules can allow direct imaging of metabolic activity and drug targets using the exquisite sensitivity of positron emission tomography (*6*, *7*).

Although strategies for aromatic fluorination developed over the past 5 years have provided access to complex aryl fluorides (*8*–*11*), there has been a notable lack of recent progress in the catalytic fluorination of aliphatic C-H bonds (*12*–*14*). Direct C-H fluorination with elemental F and electrophilic fluorinating agents, as developed by Rozen, Sandford, and Chambers (*15*–*17*), are viable and very useful methods. Metal-catalyzed direct benzylic C-H fluorination has been achieved recently with palladium catalysts and an "F^+" source (*18*). Also, advances in organocatalytic fluorination have enabled enantioselective formation of C-F bonds adjacent to a carbonyl group (*19*) or to an alcohol, in the latter case via the ring-opening of epoxides with a fluoride nucleophile (*20*). A chemo-enzymatic fluorination strategy via initial P450-mediated hydroxylation (*21*) and chemical routes involving initial decarboxylation (*22*, *23*) have also been reported. Despite this impressive progress, a method for the selective and efficient incorporation of F at unactivated C-H sites within a target molecule using fluoride ion is singularly absent from the repertoire of chemical synthesis.

The paradoxical challenge of achieving selective aliphatic fluorination lies in discovering a catalyst that is both sufficiently reactive and predictably selective to transform these ubiquitous yet unactivated sp^3 C-H bonds in the presence of other common functional groups. Such a catalyst would be particularly useful if it could use fluoride ion under convenient laboratory conditions. A strategy was suggested to us by our recent discovery of a C-H chlorination protocol using manganese porphyrin catalysts and hypochlorite ion (*24*). We considered that site-selective fluorination might be achieved if a suitable fluoride source could be found that redirected the usual biomimetic O rebound scenario (*2*) to metal-bound fluoride, in the manner of halogenating metalloenzymes such as SyrB2 that generate an oxo-chloroferrate intermediate (*25*). Thus, could a manganese fluoride capture substrate radicals generated by oxomanganese-mediated H abstraction? We report here a successful manganese-catalyzed oxidative C-H bond fluorination using fluoride ion.

We have found that a variety of simple alkanes and substituted alkanes, as well as larger natural-product molecules, can be fluorinated effectively in the presence of catalytic amounts of the bulky manganese porphyrin Mn(TMP)Cl (**1**). This oxidative aliphatic fluorination reaction is driven by iodosylbenzene as the oxo-transfer agent, using silver fluoride/tetrabutylammonium fluoride trihydrate as the fluoride source, both in stoichiometric excess (*26*). Ultra-dry conditions are not required. Results for the initial exploratory reactions of a panel of simple substrates are presented in Table 1. Cycloalkanes afforded monofluorinated products in ~50% yield. Typically, conversions were ~70%, with small amounts (15 to 20%) of alcohols and ketones also being produced. No products were detected in control experiments that omitted the manganese porphyrin or iodosylbenzene, whereas a ~2:1 ratio of oxygenated to fluorinated products was formed in the absence of tetrabutylammonium fluoride. Only oxygenated products were formed without silver fluoride (*27*). There were negligible amounts of difluorides produced at this level of conversion, probably due to the electron deficiency of the products induced by the F atom (*28*). A preliminary investigation of the substrate scope led to the results shown in Table 1 (entries 7 to 12). A range of substituted molecules, including ester, tertiary alcohol, ketone, and amide substituents, proved to be good substrates for fluorination with catalyst **1**. Fluorination of methyl cyclohexylcarboxylate (entry 7) and methyl cyclohexanol (entry 8) afforded *trans*-C3 fluorides as the major products. Monosubstituted five- and seven-membered cycloalkanes (entries 9, 10, and 12) were fluorinated exclusively at the C3 and C4 positions, respectively, suggesting subtle stereoelectronic effects on the selectivity of this reaction.

Having demonstrated that it is possible to redirect manganese-catalyzed hydroxylation to fluorination, we next aimed to apply this reaction to larger molecules. The reaction of *trans*-decalin under the same conditions afforded methylene monofluorination products with a 3.5-to-1 preference for C2 over C1 in an overall 51% yield and a 75% conversion (Fig. 1A). Very high methylene regioselectivity was observed for this substrate (>95%), similar to that observed for the manganese-catalyzed chlorination reaction we have

[1]Department of Chemistry, Frick Chemistry Laboratory, Princeton University, Princeton, NJ 08544, USA. [2]Department of Chemistry, Materials and Process Simulation Center (MC 139-74), California Institute of Technology, Pasadena, CA 91125, USA. *To whom correspondence should be addressed. E-mail: jtgroves@princeton.edu

recently reported (*24*), suggesting that a similar reactive oxo- or dioxo-manganese(V) intermediate (*29*) is responsible for the H abstraction step in both reactions.

Likewise, sclareolide, a plant-derived terpenoid with antifungal and cytotoxic activities, afforded C2 and C3 methylene-fluorinated products in an overall 58% yield (Fig. 1B). C2-fluorination was favored by nearly 3:1, probably because of the steric hindrance of the *gem*-dimethyl groups at C4. The products could be separated chromatographically. C2 selectivity has been observed for this substrate by Baran and Eschenmoser for a Rh-catalyzed amination (*30*, *31*) and by White and Chen in a Fe(pdp)/H_2O_2-mediated oxidation (*32*). In contrast, reaction of this molecule using Selectfluor (*17*) afforded an intractable mixture.

F-substituted steroids, such as dexamethasone and fluasterone, have been found to be beneficial in blocking metabolic pathways (*33*–*35*), and ^{18}F-fluorodihydrotestosterone has shown promise as a radiotracer for imaging prostate cancer in men (*36*). Because a direct, late-stage steroid fluorination protocol could greatly facilitate such applications, we sought to apply this manganese-catalyzed fluorination reaction to simple steroids. We examined the fluorination of 5α-androstan-17-one, which contains 28 unactivated sp^3 C-H bonds (Fig. 1C). Analysis of this molecule suggested that the carbonyl group would electronically deactivate ring D. Rings B and C are sterically hindered, leaving the methylene groups of the A ring as the most likely sites for H abstraction. Consistent with this analysis, and despite the complexity of the molecule, only the C2 and C3 positions in the A ring were fluorinated in an overall yield of 55% (78% of the product distribution at 70% conversion, with minor amounts of oxygenated products). The products of the reaction could be readily separated by column chromatography and structurally assigned by the diagnostic ^{19}F–nuclear magnetic resonance (NMR) spectrum and the characteristic proton J-couplings (figs. S19 to S22). A 5:1 α/β diastereoselectivity was observed for both the C2 and C3 positions, probably reflecting the steric effect of the axial methyl group at C10.

The reaction of bornyl acetate afforded a 55% yield of a single product, *exo*-5-fluoro-bornyl acetate (Fig. 1D). The characterization of this product was based on C-H correlation NMR and ^{19}F-NMR spectroscopy (figs. S27 to S30) (*37*). We anticipated that the C5 position of camphor would also be accessible, in analogy to the selectivity of P450cam (CYP101) (*38*). However, treating camphor under the standard fluorination conditions resulted in 95% recovered starting material. We attribute the low reactivity in this case to the electron-withdrawing carbonyl group, which apparently deactivates the entire molecule toward fluorination, as with the monofluoride products. These results highlight the subtle electronic effects on both the reactivity and selectivity of the fluorination reaction.

We suggest the catalytic cycle shown in Fig. 2A for this manganese porphyrin–catalyzed fluorination, although there are numerous aspects of these transformations that will require further elucidation. Oxidation of the resting Mn(TMP)F catalyst, formed in situ, would afford a reactive oxomanganese(V) species (*29*), O=Mn^{V}(TMP)F, which then abstracts a substrate H atom to produce a C-centered radical and a HO-Mn^{IV}-F rebound intermediate. Fluoride binding to separately prepared Mn^{IV}(O)(TMP) was indicated by an ultraviolet (UV) spectral shift (423 to 427 nm) that we assign to the formation of [Mn^{IV}(O)(F)(TMP)]$^-$, in analogy to the well-characterized coordination of hydroxide to Mn^{IV}(O) (*39*).

The key step in forming the fluorinated products is capture of the incipient substrate radicals either by HO-Mn^{IV}-F or a *trans*-difluoro-manganese(IV) species. There is no precedent for such a F atom transfer. In this important regard, the fluorination reaction differs from the manganese/hypochlorite chlorinating system we have described (*24*). Chloride ion is rapidly and reversibly oxidized to hypochlorite by oxoMn^{V} porphyrins (*40*). Although HOF is known (*15*), there is no evidence that fluoride is oxidized in that way under these conditions. The importance of the hypochlorite in the Mn/$^-$OCl case is illustrated by the observation of C-H bromination in the presence of hypobromite, even with a large excess of chloride ion present. We attribute the unusual methylene selectivity observed in both the fluorination and chlorination reactions to stereoelectronically enforced steric clashes between the substrate and the approaching oxoMn^{V} catalyst

Table 1. Manganese porphyrin–catalyzed fluorination of simple molecules. Reactions were run for 6 to 8 hours at 50°C under N_2 in 3:1 CH_3CN/CH_2Cl_2 solvent, 1.5 mmol substrate, 4.5 mmol silver fluoride, 6 to 8 mole % catalyst, 0.3 equivalent of tetrabutylammonium fluoride (TBAF) trihydrate, and 6 to 8 equivalents of iodosylbenzene. Yields were determined by integration of gas chromatography traces using naphthalene as the internal standard. Typical conversions were 70%. Unless otherwise noted, all major fluorination products were isolated as single compounds.

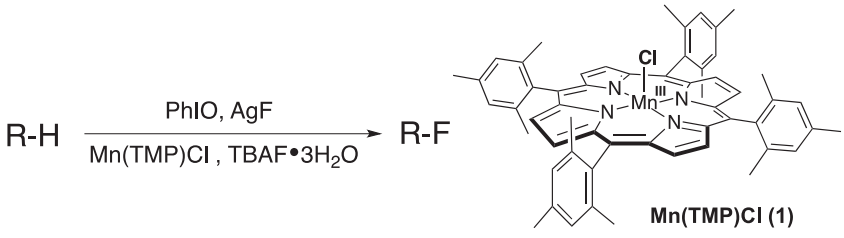

Entry	Substrate	Fluorination product	Entry	Substrate	Major fluorination product	Minor sites
1		 **2,** 49%	7		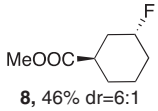 **8,** 46% dr=6:1	C4 14%
2		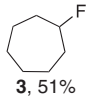 **3**, 51%	8		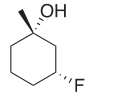 **9**, 44% dr=8:1	C4 12%
3		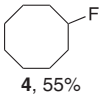 **4**, 55%	9	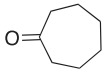	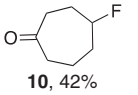 **10**, 42%	C3 11%
4		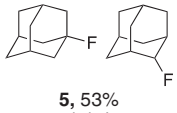 **5,** 53% 1:1.4	10	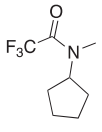	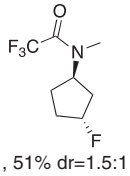 **11**, 51% dr=1.5:1	C2 <2%
5		 **6**, 49% exo: endo=5.7	11	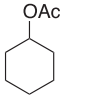	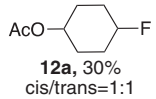 **12a,** 30% cis/trans=1:1	**12b,** C3 27% cis/trans= 2:1
6		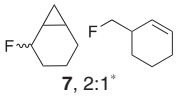 **7**, 2:1*	12	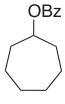	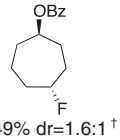 **13,** 49% dr=1.6:1†	C3 9%

*Rearranged product identified by the characteristic m-(CH_2F) peak in the mass spectrum. †Isolated as diastereomers.

(Fig. 2B). The lowest unoccupied molecular orbitals in a low-spin, d^2 oxoMn^{V} complex are expected to be the two orthogonal Mn-O π* orbitals, which would direct the approach of the scissile C-H bond into a bent π*-approach trajectory (*29*, *41*).

We conducted a number of experiments to examine this mechanistic hypothesis. Initial C-H hydroxylation was ruled out by controls showing that cyclohexanol was oxidized to cyclohexanone under these conditions. No cyclohexylfluoride was detected. Also, the hydroxyl group of 1-methylcyclohexanol is stable to the reaction conditions (Table 1, entry 8). Deuterium kinetic isotope effects (KIEs) were evaluated by the reaction of a 1:1 mixture of cyclohexane and cyclohexane-d_{12}, producing an intermolecular competitive KIE of 6.1. A similar value (5.7) was observed with a mixture of ethylbenzene and ethylbenzene-d_{10}. The large KIE indicates that C-H bond cleavage is the rate-limiting step in the reaction, consistent with typical manganese porphyrin–catalyzed hydroxylation reactions. Furthermore, reaction of norcarane, a diagnostic radical clock substrate (*2*), afforded 2-fluoronorcaranes and a significant amount of the rearranged fluorinated product, 3-fluoromethylcyclohexene (*7*), which is indicative of a C radical ring-opening process (Table 1, entry 6). The 2:1 ratio of these cyclopropylcarbinyl and homoallyl fluorides indicates a short radical lifetime of 2.5 ns and rapid trapping of the substrate radicals, given the ring-opening rate constant for the 2-norcaranyl radical of 2×10^8 M^{-1} s^{-1} (*42*). We have shown that the chlorination of norcarane with *t*-butyl hypochlorite, also involving diffusing C radical intermediates, gave a similar ratio of rearranged and unrearranged products. Further, the yields of alkyl fluorides were reduced when the reactions were run in air, indicating substrate radical trapping by O_2.

The identification of *trans*-difluoroMn^{IV}(TMP) as the likely fluorinating agent was made possible by its isolation and structural characterization. We were able to obtain pure crystals of the Mn^{IV}(TMP)F_2 by treating Mn^{IV}(TMP)Cl_2 (*43*) with excess AgF. The molecular structure of this compound showed two axially bound fluoride ions with F-Mn^{IV}-F bond lengths of 1.7931(17) and 1.7968(16) Å (Fig. 2C and tables S1 to S5). These distances are very close to those of diammonium hexafluoromanganate(IV), the only other fluoromanganese(IV) species to be structurally characterized to date (*44*).

We found that stoichiometric amounts of Mn^{IV}(TMP)F_2 could replace silver fluoride in a single-turnover C-H fluorination of cyclooctane using Mn(TMP)Cl and iodosylbenzene. A 43% yield of cyclooctyl fluoride was obtained based on added Mn^{IV}(TMP)F_2. Thermal decomposition of azo-bis-α-phenylethane to generate the phenethyl radical in the presence of Mn^{IV}(TMP)F_2 led to a 41% yield of 1-fluoroethylbenzene. These observations indicate that after initial H abstraction, Mn^{IV}(TMP)F_2 can trap the substrate radicals in the fluorine delivery step (Fig. 2A). The moderate fluorination yields from these radical trapping experiments are probably due to the falling concentration of the manganese(IV) difluoride under these conditions. Crucial roles for silver fluoride in this scenario under catalytic conditions are first to convert the added Mn(TMP)Cl to the manganese(III) fluoride form of the catalyst and then to replenish the inventory of manganese(IV) fluoride during turnover (*26*, *27*). Although a direct reaction between the substrate radicals and AgF might also be considered, the reaction between AgF and phenethyl radicals generated in situ from azo-bis-α-phenylethane afforded only trace amounts of fluorinated products.

We have explored the potential energy landscape and electronic structures of the intermediates and transition states proposed in Fig. 2A using density functional theory (DFT) computations and a polarizable continuum solvation model.

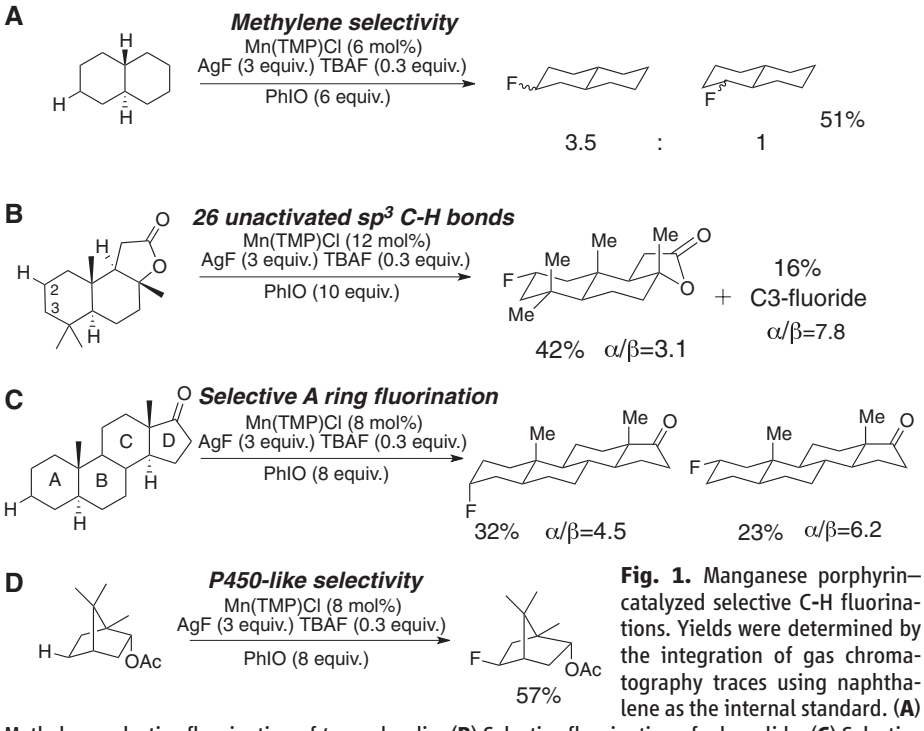

Fig. 1. Manganese porphyrin–catalyzed selective C-H fluorinations. Yields were determined by the integration of gas chromatography traces using naphthalene as the internal standard. (**A**) Methylene-selective fluorination of *trans*-decalin. (**B**) Selective fluorination of sclareolide. (**C**) Selective A-ring fluorination of 5α-androstan-17-one. (**D**) Selective 5-exo-fluorination of bornyl acetate.

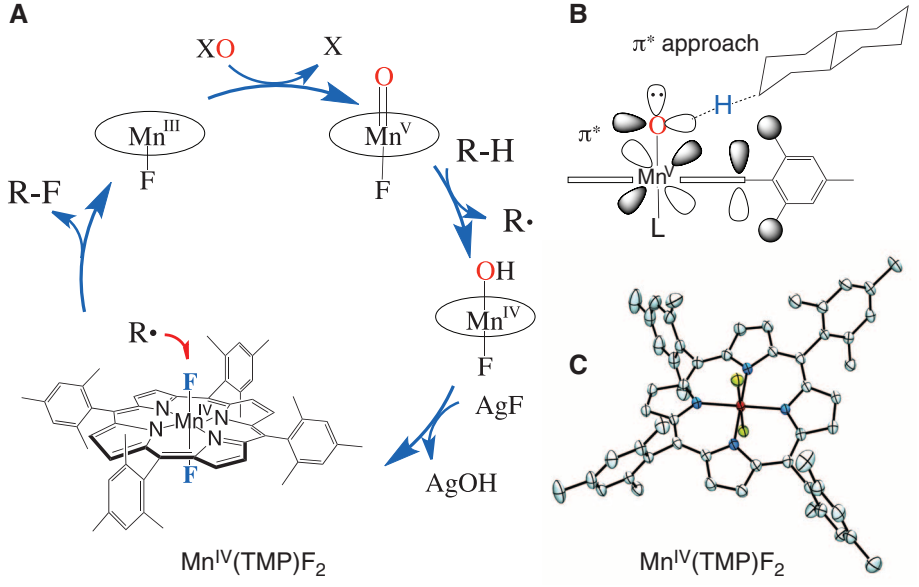

Fig. 2. (**A**) Posited catalytic cycle for manganese porphyrin–catalyzed C-H fluorination reactions. (**B**) Inferred stereoelectronics for H abstraction. (**C**) X-ray crystal structure of *trans*-Mn^{IV}(TMP)F_2 drawn at 50% probability of the electron density. Highlighted atoms are F (yellow), Mn (magenta), and N (blue) (H atoms are omitted for clarity).

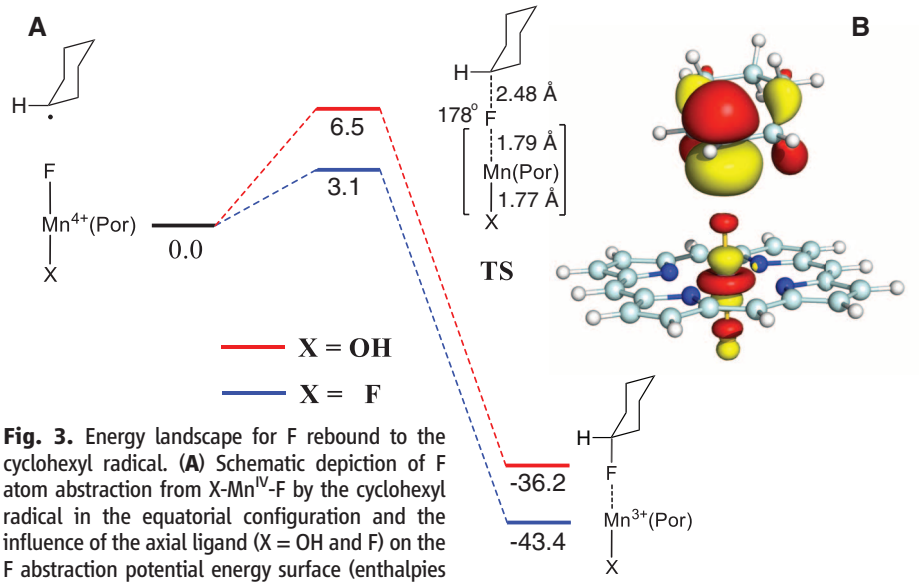

Fig. 3. Energy landscape for F rebound to the cyclohexyl radical. (**A**) Schematic depiction of F atom abstraction from X-Mn^{IV}-F by the cyclohexyl radical in the equatorial configuration and the influence of the axial ligand (X = OH and F) on the F abstraction potential energy surface (enthalpies in kilocalories per mole at 298 K). Bond distances shown are calculated for X = F. (**B**) Frontier orbital depiction of the transition state (TS) for F transfer.

We found that F atom transfer from $Mn(THP)F_2$ to a cyclohexyl radical in the equatorial configuration was predicted to occur with a surprisingly low activation barrier of only 3 kcal/mol (Fig. 3), which is very similar to the O rebound barrier for hydroxylation reactions catalyzed by oxomanganese porphyrins. A slightly higher transition state was located for the delivery of F to a cyclohexyl radical in an axial configuration (4.2 kcal/mol). Further, the calculated barrier for F transfer was ~3 kcal/mol lower for the *trans*-difluoroMn^{IV} species (Fig. 3, X = F) than for the analogous hydroxy-fluoride (Fig. 3, X = OH), implicating a much faster reaction rate for the difluoride. Consistent with this low barrier for F transfer, the transition state is very early in the reaction trajectory, showing an exceedingly long C-F distance of 2.48 Å and a Mn-F distance that is only very slightly elongated from the starting manganese(IV) difluoride (TS in Fig. 3 and fig. S31). The visible spectrum of the reaction mixture was complex, apparently due to the presence of several forms of the catalyst during turnover. However, the good yield of 1-fluoroethylbenzene from the generation of phenethyl radical in the presence of $Mn(TMP)F_2$ provides experimental support for these computational predictions that manganese(IV) fluorides of this type are excellent radical fluorinating agents.

We are encouraged by the promising initial results described here for the selective fluorination of simple hydrocarbons, substituted cyclic molecules, terpenoids, and steroid derivatives. The yields are sufficiently high and the techniques sufficiently simple that the reaction can be performed without specialized apparatus or complicated precautions, other than the normal care that should be taken whenever strong oxidants or fluoride-containing reagents are used. Given that the source of F in this one-step, one-pot protocol is fluoride ion, we anticipate the potential application of these techniques to the incorporation of ^{18}F into a wide variety of biomolecules and synthetic building blocks. Moreover, the isolation, structural characterization, and reactivity of the *trans*-difluoromanganese(IV) porphyrin, $Mn^{IV}(TMP)F_2$, suggest the existence of a rich chemistry of such transition-metal fluorides for the delivery of F substituents.

References and Notes

1. J. C. Lewis, P. S. Coelho, F. H. Arnold, *Chem. Soc. Rev.* **40**, 2003 (2011).
2. J. T. Groves, *J. Inorg. Biochem.* **100**, 434 (2006).
3. A. S. Eustáquio, D. O'Hagan, B. S. Moore, *J. Nat. Prod.* **73**, 378 (2010).
4. D. O'Hagan, C. Schaffrath, S. L. Cobb, J. T. G. Hamilton, C. D. Murphy, *Nature* **416**, 279 (2002).
5. K. Müller, C. Faeh, F. Diederich, *Science* **317**, 1881 (2007).
6. D. A. Harki, N. Satyamurthy, D. B. Stout, M. E. Phelps, P. B. Dervan, *Proc. Natl. Acad. Sci. U.S.A.* **105**, 13039 (2008).
7. S. M. Ametamey, M. Honer, P. A. Schubiger, *Chem. Rev.* **108**, 1501 (2008).
8. T. Furuya, A. S. Kamlet, T. Ritter, *Nature* **473**, 470 (2011).
9. P. P. Tang, T. Furuya, T. Ritter, *J. Am. Chem. Soc.* **132**, 12150 (2010).
10. D. A. Watson *et al.*, *Science* **325**, 1661 (2009).
11. E. Lee *et al.*, *Science* **334**, 639 (2011).
12. P. Herrmann, J. Kvicala, V. Pouzar, H. Chodounska, *Collect. Czech. Chem. Commun.* **73**, 1825 (2008).
13. S. Rozen, C. Gal, *J. Org. Chem.* **52**, 2769 (1987).
14. S. Stavber, M. Zupan, *Tetrahedron* **45**, 2737 (1989).
15. S. Rozen, *Eur. J. Org. Chem.* **2005**, 2433 (2005).
16. G. Sandford, *J. Fluor. Chem.* **128**, 90 (2007).
17. R. D. Chambers, A. M. Kenwright, M. Parsons, G. Sandford, J. S. Moilliet, *J. Chem. Soc. Perkin Trans.* **1**, 2190 (2002).
18. K. L. Hull, W. Q. Anani, M. S. Sanford, *J. Am. Chem. Soc.* **128**, 7134 (2006).
19. Y. J. Zhao, Y. H. Pan, S. B. D. Sim, C. H. Tan, *Org. Biomol. Chem.* **10**, 479 (2012).
20. J. A. Kalow, A. G. Doyle, *J. Am. Chem. Soc.* **132**, 3268 (2010).
21. A. Rentmeister, F. H. Arnold, R. Fasan, *Nat. Chem. Biol.* **5**, 26 (2009).
22. M. Rueda-Becerril *et al.*, *J. Am. Chem. Soc.* **134**, 4026 (2012).
23. F. Yin, Z. Wang, Z. Li, C. Li, *J. Am. Chem. Soc.* **134**, 10401 (2012).
24. W. Liu, J. T. Groves, *J. Am. Chem. Soc.* **132**, 12847 (2010).
25. M. L. Matthews *et al.*, *Proc. Natl. Acad. Sci. U.S.A.* **106**, 17723 (2009).
26. The excess of iodosylbenzene typically used in metalloporphyrin oxidations is due to the competing disproportionation of this reagent, which produces unreactive iodoxybenzene. The requirement for excess fluoride ion appears to derive from the stoichiometry of the fluorination reaction, which also produces hydroxide ions. AgF converts Mn-OH to Mn-F species and Ag_2O.
27. The need for both AgF and tetrabutyammonium fluoride apparently derives from the limited solubility of AgF in the reaction medium and the need for a higher fluoride ion concentration than can be maintained by AgF alone. The UV-visible λ_{max} observed for $(TMP)Mn^{III}$-Cl (**1**) (475 nm) changed immediately to that of a mixture of $(TMP)Mn^{III}$-F (453 nm) and $[(TMP)Mn^{III}(F)_2]^-$ (440 nm) under the reaction conditions.
28. The high selectivity for monofluorination, the low reactivity of C-H bonds near carbonyl groups, and the limited reactivity of the solvents as well as the tetrabutylammonium ion seem to reflect a very strong polar effect in the C-H bond cleavage step in this reaction.
29. N. Jin, M. Ibrahim, T. G. Spiro, J. T. Groves, *J. Am. Chem. Soc.* **129**, 12416 (2007).
30. T. Newhouse, P. S. Baran, *Angew. Chem. Int. Ed.* **50**, 3362 (2011).
31. K. Chen, A. Eschenmoser, P. S. Baran, *Angew. Chem. Int. Ed.* **48**, 9705 (2009).
32. M. S. Chen, M. C. White, *Science* **327**, 566 (2010).
33. J. P. Bégué, D. Bonnet-Delpon, *J. Fluor. Chem.* **127**, 992 (2006).
34. N. Houstis, E. D. Rosen, E. S. Lander, *Nature* **440**, 944 (2006).
35. R. I. Scheinman, P. C. Cogswell, A. K. Lofquist, A. S. Baldwin Jr., *Science* **270**, 283 (1995).
36. P. B. Zanzonico *et al.*, *J. Nucl. Med.* **45**, 1966 (2004).
37. L. F. Lourie *et al.*, *J. Fluor. Chem.* **127**, 377 (2006).
38. I. Schlichting *et al.*, *Science* **287**, 1615 (2000).
39. J. T. Groves, M. K. Stern, *J. Am. Chem. Soc.* **110**, 8628 (1988).
40. T. P. Umile, D. Wang, J. T. Groves, *Inorg. Chem.* **50**, 10353 (2011).
41. N. Jin, D. E. Lahaye, J. T. Groves, *Inorg. Chem.* **49**, 11516 (2010).
42. K. Auclair, Z. B. Hu, D. M. Little, P. R. Ortiz De Montellano, J. T. Groves, *J. Am. Chem. Soc.* **124**, 6020 (2002).
43. L. Kaustov, M. E. Tal, A. I. Shames, Z. Gross, *Inorg. Chem.* **36**, 3503 (1997).
44. S. Kaskel, J. Strähle, *Z. Anorg. Allg. Chem.* **623**, 1259 (1997).

Acknowledgments: We are grateful to NSF (grants CHE-0616633 and CHE-1148597 to J.T.G.) for support of this research. DFT calculations, hydrocarbon C-H activation, and the CalTech-Princeton collaboration were supported by the Center for Catalytic Hydrocarbon Functionalization, an Energy Frontier Research Center, U.S. Department of Energy, Office of Science, Basic Energy Sciences, under award no. DE-SC0001298 to W.A.G. and J.T.G. A patent application has been filed through Princeton University on methods and catalysts presented in this paper. We thank S. Semproni for assistance with the x-ray crystal structure of $Mn^{IV}(TMP)F_2$, data for which are available free of charge from the Cambridge Crystallographic Data Centre under reference no. CCDC 893742.

Supplementary Materials

www.sciencemag.org/cgi/content/full/337/6100/1322/DC1
Materials and Methods
Figs. S1 to S31
Tables S1 to S6
References (*45*–*58*)

23 March 2012; accepted 26 July 2012
10.1126/science.1222327